

Article

Selective H₂ Evolution and CO₂ Absorption in Electrolysis of Ethanolamine Aqueous Solutions

Satoshi Fukada *, Ryosuke Sakai, Makoto Oya and Kazunari Katayama

Department of Advanced Energy Engineering Science, Kyushu University, Fukuoka 816-8581, Japan; sfukada@nucl.kyushu-u.ac.jp (R.S.); moyaa@aees.kyushu-u.ac.jp (M.O.); katayama.kazunari.947@m.kyushu-u.ac.jp (K.K.)

* Correspondence: fukada.satoshi.334@m.kyushu-u.ac.jp; Tel.: +81-92-583-7608

Abstract: Selective H₂ evolution and CO₂ absorption in several ethanolamine aqueous solutions are comparatively investigated using a new electrolysis reactor. H₂ bubbles are generated from a cathode in any ethanolamine electrolyte, and its experimental gas evolution rates are correlated by Faraday's first rule. No or smaller amounts of CO₂ and N₂ bubbles than stoichiometric ones are generated on an anode through the reaction between hydroxide ions and ethanolamine ones. No CO or O₂ is observed in the system exhaust, and most of the CO₂, along with N₂, is still absorbed in ethanolamine aqueous solutions with the addition of KOH and/or HCOOH under high pH conditions. Variations of the concentrations of coexisting ions dissolved in the electrolytes of mono- or tri-ethanolamine (MEA or TEA) and ethylenediamine (EDA) solutions with CO₂ absorption are calculated using the equilibrium constants to relate the concentrations of solute ions. Electric resistivities of the ethanolamine aqueous solutions are correlated by the pH value and are analyzed in terms of equilibrium constants among the concentrations of coexisting ions. Conditions of the MEA electrolyte to achieve high-performance electrolysis is discussed for selective H₂ generation.

Keywords: electrolysis; hydrogen; ethanolamine; carbon dioxide absorption



Citation: Fukada, S.; Sakai, R.; Oya, M.; Katayama, K. Selective H₂ Evolution and CO₂ Absorption in Electrolysis of Ethanolamine Aqueous Solutions. *Separations* **2023**, *10*, 578. <https://doi.org/10.3390/separations10110578>

Academic Editor: Federica Raganati

Received: 30 October 2023

Revised: 11 November 2023

Accepted: 18 November 2023

Published: 20 November 2023



Copyright: © 2023 by the authors. Licensee MDPI, Basel, Switzerland. This article is an open access article distributed under the terms and conditions of the Creative Commons Attribution (CC BY) license (<https://creativecommons.org/licenses/by/4.0/>).

1. Introduction

Hydrogen (H₂) is a promising secondary energy source in the near future. Because H₂ is not present in natural resources, two major production methods are developed and put into industrial use. One is H₂ production by electrolysis of alkaline water or relevant aqueous solutions, which uses an expensive proton exchange membrane (PEM) to separate electrolytes between two electrodes. Aqueous solutions of alkali chloride (NaCl or KCl) are also used for the production of NaOH or KOH and Cl₂ for industrial uses. Then, H₂ is generated as another by-product. H₂ is separately generated from Cl₂ using an anion exchange membrane (AEM) and two separate electrodes [1]. However, H₂ purification is necessary for industrial high-grade products [2]. Another H₂ production method is the steam-reformation reaction or partial oxidation from natural resources, such as hydrocarbons of methane, naphtha and coal. By-product carbon monoxide (CO), along with H₂ included in the combustion gas, is recovered from exhaust gas to be utilized as industrial raw materials for synthesizing carbonyl groups. Carbon dioxide (CO₂) generated is necessary to be recovered without exhausting the atmospheric environment. Most CO₂ is recovered by the pressure swing adsorption (PSA) process or liquid film absorption by ethanolamine solutions in H₂ production sites. Thus, industrial H₂ production ways are closely related to the processes of H₂ purification and CO₂ recovery. Its selective production and recovery become a key for effective H₂ production in place of conventional technology methods.

Here, attention is focused on alkaline water electrolysis for small-scale H₂ production plants. Constituents of H₂ and O₂ in water electrolyte are produced from cathode and anode separated with a solid polymer film [3,4]. It is necessary not to mix the two gas

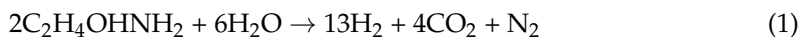
products. In order to advance H₂ production more effectively, a new technology is tested to evolve only H₂ with the use of a nickel–hydroxide electrode for the anode. Oxygen is absorbed by the oxidation reaction from Ni(OH)₂ electrodes to NiOOH during electrolysis [5]. Then, oxygen is recovered by the reverse reaction to Ni(OH)₂ in the outside of the reactor. Although the products of H₂ and O₂ are completely separated by electrolysis, two independent processes of water electrolysis and electrode regeneration are necessary for continuous H₂ production. In the present study, a new electrolysis process is tested using ethanolamine aqueous solutions. The ethanolamine aqueous solution is a candidate for materials that are widely used to recover CO₂ from various exhaust gases. High CO₂ capacities are expected. It is expected that selective H₂ generation and CO₂ absorption can be achieved using electrolysis of ethanolamine aqueous solutions. Enhancement of H₂ production efficiency without CO₂ or CO exhaustion is expected. So, it is necessary to fully understand the overall mechanism of H₂ transfer and effective CO₂ recovery from multicomponent amine mixtures. As our first trial to achieve this, attention is focused on the combination of H₂ production by electrolysis of ethanolamine aqueous solutions and CO₂ recovery in them at the same time. In the present study, H₂ generation and simultaneous CO₂ generation/absorption by the electrolysis of several alkanolamines aqueous solutions are investigated in order to make clear not only the relation between the overall transfer mechanism of electrolysis products and electrical resistivities but also CO₂ absorption/desorption rates in ethanolamine aqueous solutions. A small-scale apparatus for selective H₂ production without further product purification is targeted here.

Ethanolamine is the most promising absorber among several alkanolamines to separate CO₂ and other gas components, such as CO and CH₄, in industrial exhaust gases. Usually, CO₂ is selectively recovered from exhaust gas using gas absorption towers, where aqueous alkanolamines and exhaust gas flow downward and upward counter-currently around room temperature, respectively [6]. Then, another CO product is recovered from the top as raw materials for chemical synthesis. Amine solutions after CO₂ absorption are regenerated using another gas desorption tower, which is operated at higher temperatures. Research on CO₂ absorption and desorption was previously performed using several kinds of ethanolamines [7–11]. Although their solution mechanism has been investigated from various viewpoints in terms of chemical engineering keywords [8,9], the difference between physical absorption and chemical absorption is not sufficiently quantified and clarified. In addition, the effects of other ions or molecules coexisting in alkanolamine solutions are not understood sufficiently. In the present study, CO₂ absorption in several amine solvents is comparatively investigated using electrolysis reactors of three amine aqueous solutions: (1) mono-ethanolamine (MEA), with the molecular form C₂H₄OHNH₂ described as R₁NH₂ (R = C₂H₄OH), and which is one of the primary alkanolamines, (2) tri-ethanolamine (TEA), which is (C₂H₄OH)₃N or R₃N and one of the tertiary alkanolamines and (3) ethylenediamine (EDA), which molecular form is C₂H₄(NH₂)₂, and it is a primary amine without any hydroxyl group. In addition, the [H⁺] ion concentration in the three amines aqueous solutions is controlled to an arbitral value using KOH and HCOOH (or (COOH)₂) agents for pH adjustment. The combination of CO₂ absorption and H₂ generation by electrolysis using the three amine solutions is experimentally investigated here. The H₂ evolution rates on an SS316 cathode plate and CO₂ and N₂ ones on a graphite anode plate are measured. It is investigated as to how different the H₂ evolution rates and N₂ or CO₂ ones are among the three kinds of amine compounds under various pH conditions. Electric resistances and gas evolution rates in the electrolysis of the three amine solutions are determined. Aside from this, CO₂ absorption rates in the three amine solutions during electrolysis are also determined as a function of the pH value. The present study may give useful information on small-scale H₂ production by electrolysis and simultaneous CO₂ absorption using amine solutions.

2. Analysis

2.1. Electrolysis of Aqueous Amine Solutions

If the current efficiency is assumed to be 1 in the electrolysis of alkaline water, the relations between the molar generation rates of H₂ and O₂ gases, W_{H_2} and W_{O_2} , and current, I , are expressed as $W_{H_2} = I/2F$ and $W_{O_2} = I/4F$ using the Faraday constant, F . Consequently, the total gas generation rate is expressed by $W_{tot} = W_{H_2+O_2} = 3I/4F$. On the other hand, when an MEA aqueous solution is electrolyzed [9], it is expected that H₂, CO₂ and N₂ are separately generated on the cathode and anode by the overall reaction:



Equation (1) means that the reaction of $26H_2O + 26e^- = 13H_2 + 26OH^-$ proceeds on cathode and the reaction of $2C_2H_4OHNH_2 + 26OH^- = 4CO_2 + N_2 + 20H_2O + 26e^-$ does on anode under high pH conditions. No CO and O₂ are generated in the usual electrolysis process of MEA. The stoichiometric generation rates of gases evolved from MEA are $W_{H_2} = I/2F$, $W_{CO_2} = 2I/13F$ and $W_{N_2} = I/26F$. The stoichiometric H₂ generation rate is 6.5 H₂-mol/MEA-mol from Equation (1). The ratio of the gas generation rates is H₂:CO₂:N₂ = 13:4:1. The total generation rate is $W_{tot} = W_{H_2+CO_2+N_2} = 9I/13F$. However, when all of the CO₂ and N₂ generated on the anode is physically or chemically absorbed in the MEA solution, only H₂ evolution may be observed on the cathode as gas bubbles. This means $W_{tot} \cong I/2F$. Similarly, the W_{tot} and W_{H_2} values for the TEA aqueous solution are $W_{tot} = 41I/56F$ and $W_{H_2} = I/2F$ from Faraday's first law. The stoichiometric H₂ generation rate of TEA is 14 H₂-mol/TEA-mol. The W_{tot} and W_{H_2} values for the EDA aqueous solution are estimated as $W_{tot} = 11I/16F$ and $W_{H_2} = I/2F$. The stoichiometric H₂ generation rate of EDA is 8 H₂-mol/EDA-mol.

2.2. CO₂ Dissolution into Amine Aqueous Solutions

It depends on the chemical conditions of solutes and whether CO₂ bubbles evolved from the electrode or not. When CO₂ gas bubbles come into contact with an aqueous solution of primary amine MEA, its overall solution process is divided into two stages: a physical diffusion process and a chemical reaction. Amine solutions absorb CO₂ physically at first, and then its physical state moves to the next chemical one. The molar concentration of CO₂ under the physical diffusion state is expressed by [CO₂], and the chemical ones are described according to their respective ionic states as follows: [HCO₃⁻], [CO₃²⁻], [R₁NHCOO⁻] and [R₁NH₃⁺]. Several reactions occur among molecules or ions dissolved in solutions. When a primary amine, such as MEA, absorbs CO₂ chemically, it is considered that the chemical dissolution reaction advances through a zwitterion state of R₁NH₂ + COO⁻ to a carbamate of R₁NHCOOH [12]. The overall reaction is described by $2R_1NH_2 + CO_2 = R_1NHCOO^- + R_1NH_3^+$. Therefore, MEA has three types of CO₂ loading capacities: carbonic (HCO₃⁻), bicarbonic acid (CO₃²⁻) and carbamate (R₁NHCOO⁻). The chemical solution process proceeds also in the case of the secondary amine (R₂NH). On the other hand, the tertiary amine of TEA does not form any carbamate but only bicarbonate ions because of the absence of an N–H bond in its molecule structure. Consequently, it forms only carbonic or bicarbonic acid.

It is assumed that the overall rate of CO₂ absorption from gas bubbles into the physical state is limited by the two steps: (1) diffusion in a liquid boundary layer existing outside bubbles during gas contact with solute and (2) the first-order reaction rate depending on the dissolved CO₂ concentration, which means its rate is in proportion to [CO₂], as follows:

$$V \frac{d[CO_2]}{dt} = k_{abs} A ([CO_2]_s - [CO_2]) - k_1 V [CO_2] \quad (2)$$

All symbols used in the present paper are explained in nomenclature. It is considered that the CO₂ mass-transfer rate constant through a liquid boundary layer around CO₂ gas bubbles is expressed by k_{abs} of the first term in Equation (2) according to the liquid film

theory [13]. The reaction rate from a physical state to the chemical state per unit liquid volume is in proportion to the rate constant k_1 , which is the second term of Equation (2). It is assumed that the bulk $[CO_2]$ concentration in Equation (2) is uniform all over the liquid volume of solutions during short contact time because the time when gas bubbles pass through the MEA solution is much shorter than the $[CO_2]$ conversion time from the physical state to the chemical one. If one needs to take into consideration variations of the R_1NH_2 concentration with the reaction progressing, it is necessary to replace the chemical reaction term of $k_1V[CO_2]$ with $k_2V[R_1NH_2][CO_2]$. The first reaction rate constant, k_1 , is then replaced by the secondary rate one, k_2 . The value of $[CO_2]_S$ is constant regardless of time, and it depends on only the CO_2 partial pressure of gas bubbles. Usually, Henry's law holds between $[CO_2]_S$ and CO_2 partial pressure in the gas phase [8,13]. Equation (2) is solved with the use of the initial time condition of $[CO_2] = 0$ at $t = 0$ under the assumption of the constant $[CO_2]_S$ condition as follows:

$$\frac{[CO_2]}{[CO_2]_S} \left(= \frac{y_{CO_2,out}}{y_{CO_2,in}} \right) = \frac{k_{abs}A}{k_{abs}A + k_1V} \left\{ 1 - \exp\left(-\frac{k_{abs}A + k_1V}{V}t\right) \right\} \quad (3)$$

Equation (3) can be approximated by a linear rate equation of $[CO_2]/[CO_2]_S \cong k_{abs}At/V$ in an initial time range, and its absorption rate is limited by the physical absorption process. Contrarily, the ratio of the g_7 concentration in the evolved gas to the saturated one approaches a constant after sufficient contact time while bubbling, and the CO_2 molar fraction ratio on the left-hand side of Equation (3) becomes equal to a constant defined as $k_{abs}A/(k_{abs}A + k_1V)$ under the steady state. It is considered that k_{abs} may be independent of the kind of amines, and only k_1 depends on it. When the value of k_1V is much larger than that of $k_{abs}A$, the $y_{CO_2,out}/y_{CO_2,in}$ ratio of evolved gas approaches 0. On the contrary, the ratio on the left-hand side approaches unity when k_1V is much smaller than $k_{abs}A$, which means a very low chemical solution rate.

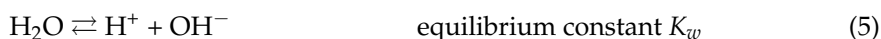
There is less chemical absorption site for CO_2 in the molecular structure of TEA. Therefore, the chemical absorption amount of CO_2 in TEA is limited to those of HCO_3^- and CO_3^{2-} . On the contrary, the EDA aqueous solution has the six chemical absorption states of $(CH_2)NH_2NHCOO^-$, $(CH_2)_2(NHCOO^-)_2$, $(CH_2)_2NH_2NH_3^+$, $(CH_2)_2(NH_3)^{2+}$ as shown in Appendix A in addition to HCO_3^- and CO_3^{2-} . Further, when EDA reacts chemically with CO_2 , the product of 2-imidazolinone or ethylene urea is generated by the reaction [14]:

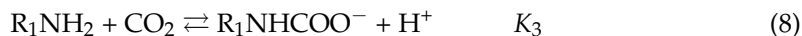


The Reaction (4) is irreversible. Therefore, it is expected that EDA also has a higher CO_2 loading capacity than others.

2.3. Analysis of Chemical Equilibrium among Ions in Amine Solutions

At first, CO_2 is absorbed physically in an MEA solution, and the concentration of free CO_2 dissolved in a solution is described by $[CO_2]$. The same physical absorption state appears also in TEA and EDA ones. Then, the free CO_2 reacts with MEA and OH^- dissolved in water. KOH and HCOOH added for pH adjustment are also present together with K^+ , H^+ , and $COOH^-$ ions in the solution. The reaction between MEA and CO_2 proceeds via zwitterion ($R_1NH_2 + COO^-$) to carbonic acid ($R_1NHCOOH$). Therefore, CO_2 and R_1NH_2 in aqueous solutions change to ions of HCO_3^- , CO_3^{2-} , R_1NHCOO^- , or $R_1NH_3^+$, which are under the chemical solution conditions. Thus, chemical CO_2 dissolution has been accomplished in an aqueous MEA + KOH + HCOOH solution. If the concentrations of all ions dissolved in a MEA aqueous solution reach equilibrium, the reactions among them are expressed using the six equilibrium constants defined by K_i ($i = w, 1\sim5$) as follows:





Reactions (5), (7), (9) and (10) are considered to be reversible and reach instantaneous equilibrium because they involve only a proton transfer. Reaction (7) is also described as $\text{HCO}_3^- + \text{OH}^- = \text{CO}_3^{2-} + \text{H}_2\text{O}$. In contrast, the remaining Reactions (6) and (8) are nearly reversible due to finite reaction rates [13,15]. Judging from the previous data on reaction rates between CO_2 and OH^- or MEA [16], it is considered that Reactions (6) and (8) also reach equilibrium within a short contact time range. The equilibrium constants of Reactions (5)–(10), K_w , K_1 , K_2 , K_3 , K_4 and K_5 , are determined based on the thermodynamic values of the enthalpy and entropy changes in the references as follows [16,17]:

$$K_w = f_{\text{H}^+} [\text{H}^+] f_{\text{OH}^-} [\text{OH}^-] = 10^{-14} \quad (11)$$

$$K_1 = \frac{f_{\text{HCO}_3^-} [\text{HCO}_3^-]}{f_{\text{CO}_2} [\text{CO}_2] f_{\text{OH}^-} [\text{OH}^-]} = 10^{7.65} \quad (12)$$

$$K_2 = \frac{f_{\text{CO}_3^{2-}} [\text{CO}_3^{2-}] f_{\text{H}^+} [\text{H}^+]}{f_{\text{HCO}_3^-} [\text{HCO}_3^-]} = 10^{-10.33} \quad (13)$$

$$K_3 = \frac{f_{\text{R}_1\text{NHCOO}^-} [\text{R}_1\text{NHCOO}^-] f_{\text{H}^+} [\text{H}^+]}{f_{\text{R}_1\text{NH}_2} [\text{R}_1\text{NH}_2] f_{\text{CO}_2} [\text{CO}_2]} = 10^{-4.74} \quad (14)$$

$$K_4 = \frac{f_{\text{R}_1\text{NH}_3^+} [\text{R}_1\text{NH}_3^+]}{f_{\text{R}_1\text{NH}_2} [\text{R}_1\text{NH}_2] f_{\text{H}^+} [\text{H}^+]} = 10^{9.74} \quad (15)$$

$$K_5 = \frac{f_{\text{H}^+} [\text{H}^+] f_{\text{COOH}^-} [\text{COOH}^-]}{f_{\text{HCOOH}} [\text{HCOOH}]} = 10^{-3.75} \quad (16)$$

Electrolytic neutrality holds in the whole $\text{KOH} + \text{HCOOH} + \text{R}_1\text{NH}_2$ aqueous solution. Consequently, the following formula holds true:

$$[\text{K}^+] + [\text{H}^+] + [\text{R}_1\text{NH}_3^+] = [\text{OH}^-] + [\text{HCO}_3^-] + 2[\text{CO}_3^{2-}] + [\text{R}_1\text{NHCOO}^-] + [\text{COOH}^-] \quad (17)$$

The respective total concentrations of R_1NH_2 , CO_2 and HCOOH in the aqueous solution, $[\text{R}_1\text{NH}_2]_0$, $[\text{CO}_2]_0$ and $[\text{HCOOH}]_0$, are defined as follows:

$$[\text{HCOOH}]_0 = [\text{HCOOH}] + [\text{COOH}^-] \quad (18)$$

$$[\text{R}_1\text{NH}_2]_0 = [\text{R}_1\text{NH}_2] + [\text{R}_1\text{NH}_3^+] + [\text{R}_1\text{NHCOO}^-] \quad (19)$$

$$[\text{CO}_2]_0 = [\text{CO}_2] + [\text{R}_1\text{NHCOO}^-] + [\text{HCO}_3^-] + [\text{CO}_3^{2-}] \quad (20)$$

When any activity coefficients included in Equations (11)–(16) are described as f_k , the material balance equations of Equations (17) and (20) are correlated in terms of $[K^+]$, $[H^+]$, $[CO_2]$, $[CO_2]_0$, $[HCOOH]_0$ and $[R_1NH_2]_0$ into the two relations as follows:

$$[K^+] + [H^+] + \frac{K_4 f_{R_1NH_2} f_{H^+} [H^+] [R_1NH_2]_0}{f_{R_1NH_3^+} \left\{ 1 + \frac{K_4 f_{R_1NH_2} f_{H^+} [H^+]}{f_{R_1NH_3^+}} + \frac{K_3 f_{R_1NH_2} f_{CO_2} [CO_2]}{f_{R_1HCOO^-} f_{H^+} [H^+]} \right\}} = \frac{K_5 f_{HCOOH} [HCOOH]_0}{f_{H^+} f_{COOH^-} [H^+] + K_5 f_{HCOOH}} + \frac{K_W}{f_{H^+} f_{OH^-} [H^+]} + f_{CO_2} [CO_2] \times \left\{ \frac{K_W K_1}{f_{H^+} f_{HCO_3^-} [H^+]} + \frac{2K_W K_1 K_2}{f_{CO_3^{2-}} f_{H^+}^2 [H^+]^2} + \frac{K_3 f_{R_1NH_2} [R_1NH_2]_0}{f_{H^+} f_{R_1NHCOO^-} [H^+] \left\{ 1 + \frac{K_4 f_{R_1NH_2} f_{H^+} [H^+]}{f_{R_1NH_3^+}} + \frac{K_3 f_{CO_2} f_{R_1NH_2} [CO_2]}{f_{H^+} f_{R_1NHCOO^-} [H^+]} \right\}} \right\} \quad (21)$$

$$\frac{[CO_2]_0}{[CO_2]} = 1 + \frac{K_W K_1 f_{CO_2}}{f_{HCO_3^-} f_{H^+} [H^+]} + \frac{K_W K_1 K_2 f_{CO_2}}{f_{CO_3^{2-}} f_{H^+}^2 [H^+]^2} + \frac{K_3 f_{R_1NH_2} f_{CO_2} [R_1NH_2]_0}{f_{H^+} f_{R_1NHCOO^-} [H^+] \left\{ 1 + f_{R_1NH_2} \left(\frac{K_4 f_{H^+} [H^+]}{f_{R_1NH_3^+}} + \frac{K_3 f_{CO_2} [CO_2]}{f_{H^+} f_{R_1NHCOO^-} [H^+]} \right) \right\}} \quad (22)$$

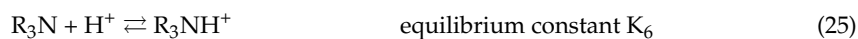
The activity coefficients f_k for each ion X_k ($k = 1 \sim N$) are determined based on the Debye-Hueckel theory [18] as the following relation:

$$J = \frac{1}{2} \sum_{k=1}^N [X_k] z_k^2 \quad (23)$$

$$\log_{10} f_k = -\frac{Az_k^2 \sqrt{J}}{1 + Ba\sqrt{J}} \quad (24)$$

where the constants are given as $A = 0.51 \text{ (mol/dm}^3\text{)}^{-0.5}$, $B = 0.33 \times 10^{10} \text{ (mol/dm}^3\text{)}^{-0.5}/m$, and a is an average ion diameter [19]. Since the values of $[H^+]$ and $[CO_2]$ are determined from Equations (21) and (22) by means of the least squared method, the remaining ion concentrations of $[OH^-]$, $[HCO_3^-]$, $[CO_3^{2-}]$, $[R_1NHCOO^-]$, $[R_1NH_3^+]$ and $[COOH^-]$ are calculated as a function of $[K^+]$, $[R_1NH_2]_0$, $[CO_2]_0$ and $[HCOOH]_0$. Since KOH is a strong acid, its dissociation degree can be approximated as unity. This means that the relation of $[KOH]_0 = [K^+]$ holds true. Thus, all ion concentrations of $[H^+]$, $[OH^-]$, $[HCO_3^-]$, $[CO_3^{2-}]$, $[R_1NHCOO^-]$, $[R_1NH_3^+]$ and $[COOH^-]$ along with $[CO_2]$, $[R_1NH_2]$ and $[HCOOH]$ are determined from the total concentrations of $[CO_2]_0$, $[KOH]_0$, $[HCOOH]_0$ and $[R_1NH_2]_0$ based on the electric neutral balance equation. The H^+ ion concentration index, $pH (= -\log_{10} [H^+])$, at the initial condition is controlled by both $[KOH]_0$ and $[HCOOH]_0$, and the rest of the ion concentrations are determined as a function of $[CO_2]_0$ using Equations (11)–(16).

When CO_2 is in contact with aqueous TEA + KOH + HCOOH solutions in place of MEA + KOH + HCOOH solutions, the equilibrium relations of Reactions (8) and (9) are replaced by the following equations:



$$K_6 = \frac{f_{R_3NH^+} [R_3NH^+]}{f_{R_3N} [R_3N] f_{H^+} [H^+]} = 10^{7.88} \quad (26)$$

Since the tertiary amine of TEA has no N–H bond in its molecular structure, ethanol carbamic acid is not generated differently from the case of the MEA solution of Equation (8). Therefore, the CO_2 absorption capacity of the TEA solution is limited to HCO_3^- and CO_3^{2-} . Similarly, when CO_2 is absorbed in the EDA solution in place of MEA and TEA one, the replacement equilibrium equations of Reactions (8) and (9) are shown in Appendix A. When EDA is used for the aqueous amine electrolyte in place of MEA or TEA, the equilibrium is achieved among several ions shown in Appendix A.

If the oxalic acid $(COOH)_2$ is used for the pH adjustment in place of the formic acid HCOOH, the corresponding analytical equations are given in Appendix B.

3. Experimental

Figure 1 shows a schematic diagram of the experimental apparatus. A specified amount (3.00 dm^3) of a fresh amine aqueous solution for each experiment is filled in an acrylic square vessel, and two electrodes are inserted. Open space between aqueous solution surfaces in the acrylic vessel

and its lid is set as narrow as possible to make the time response fast. A partition made of an acrylic plate is set in the open space to separate two electrodes and evolved gases. The anode electrode plate is made of graphite having a volume resistivity $\rho_C = 1.64 \times 10^{-5} \Omega\text{m}$, and the cathode electrode one is made of SS316 having $\rho_{SS} = 7.2 \times 10^{-7} \Omega\text{m}$. The thickness of two plate electrodes, δ , is 1.0 mm, their area, A , is 176.3 cm², and the distance between the anode and the cathode, l , is 13.6 cm. Since the resistances of the anode and the cathode are much lower than the overall resistance of amine electrolytes (0.5–10 Ω), the resistances of the two electrodes can be neglected. Three kinds of amine solutions are tested here. The three amines are MEA, TEA and EDA of special grade. The purity of the three amines is >99.0+%. The experiment is performed in such a way that respective amine gram concentrations are the same as 200 g/dm³ regardless of MEA, TEA and EDA aqueous solutions. This is because the gas generation rates of H₂, CO₂ and N₂ per unit volume of each amine are expected to be almost the same among the three amine solutions with different molecular weights. The stoichiometric H₂ generation rates for the three amines are 6.5 mol-H₂/mol-MEA, 14 mol-H₂/mol-TEA and 8 mol-H₂/mol-TEA if the current efficiency is assumed to be 1. The expected maximum generation rate is reduced to almost the same value of 0.10 mol-H₂/g-amine regardless of MEA, TEA and EDA. The amine molar concentration used in the experiment is 3.27 mol/dm³ for MEA, 1.35 mol/dm³ for TEA and 3.30 mol/dm³ for EDA. The pH value of each amine solution at the initial state before electrolysis or CO₂ + Ar gas bubbling is controlled to a specified one by using potassium hydroxide (KOH), formic acid (HCOOH) or oxalic acid (COOH)₂. The molar concentrations of KOH and HCOOH are [KOH]₀ = 0.18 M and [HCOOH]₀ = 0.17 M, respectively. The initial pH value is controlled between 7 and 13. Arbitral electric current and voltage can be applied between two electrodes, and variations of the overall resistances with current are determined. No corrosion was observed on two electrodes after all the electrolysis experiments were finished.

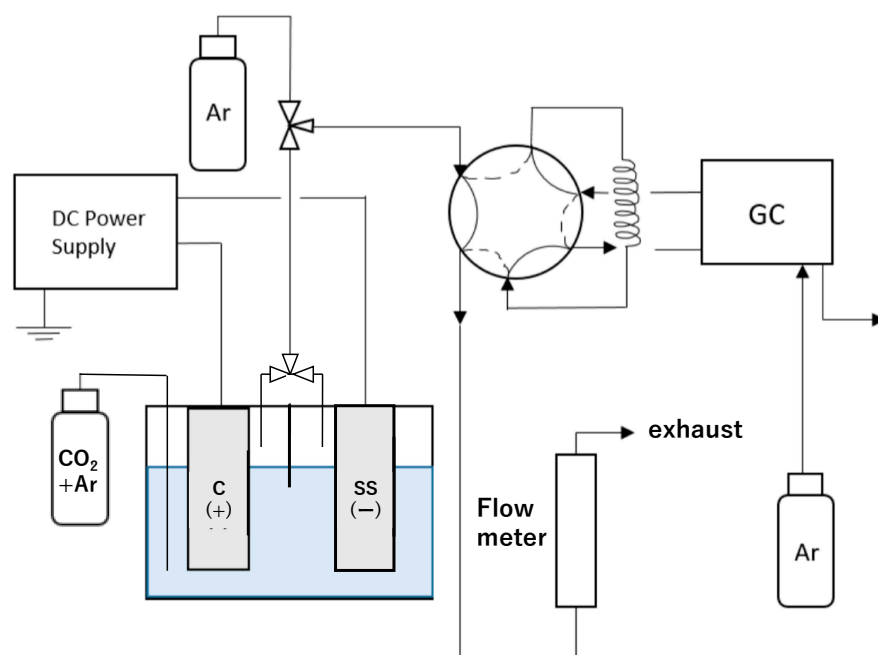


Figure 1. A schematic diagram of the experimental apparatus.

Four kinds of measurements are carried out: (1) measurement of overall resistances and gas evolution rates from two electrodes during electrolysis of MEA (or TEA, EDA) + KOH + HCOOH solutions, (2) measurement of the H₂, CO₂ and N₂ molar fractions in the gaseous phase evolved from several amine electrolyte solutions during electrolysis, (3) the pH measurement during electrolysis with time passage and numerical analysis on variations of ion concentrations in solutions, and (4) measurement of CO₂ absorption rates under the supply of a constant concentration and a flow rate of CO₂ + Ar gas bubbles during electrolysis.

The flow rates of gases evolved from the anode and cathode were measured by a soap film flowmeter, and the concentrations of the molecular species, such as H₂, O₂, CO₂, CO, CH₄ and N₂ in evolved gas, are detected separately by gas chromatography. Electrolyte temperature was measured regularly, and its average temperature was 21 °C. Isotherm conditions were kept throughout the

experiment with air cooling. Effects of reaction heat during electrolysis are supposed to be negligibly small under the present experimental conditions.

4. Results and Discussion

Since the flow rate of gas that evolved from the anode was negligibly low, attention was focused on the total flow rate of gas that evolved from two electrodes after the space plate separating the two electrodes was removed. Figure 2 shows the total gas evolution rates as a function of current in the case of electrolysis of six different concentrations of the amine aqueous solutions and the alkali KOH solution. The experiment is repeated under the conditions of different amine solutions and pH conditions. At least seven data for each symbol in Figure 2 are plotted under the same pH and amine conditions. The pH value is almost constant between 12.7 and 13.2 for the amine + KOH solution and between 10.4 and 10.9 for the amine + KOH + HCOOH solution throughout the electrolysis experiment. In addition to the six experiments, when the KOH solution (pH 13.0) without amine is electrolyzed, H₂ and O₂ gases evolved on the cathode and anode as expected. No CO₂ and CO are generated from the anode electrode, which is made of graphite. This is assured by gas chromatographic analysis of evolved gas. Experimental data and estimation in the case of the KOH solution are shown by ⊗ and a chained line in the Figure, respectively. The total evolution rates are compared with a chain line of $W_{H_2+O_2} = 3I/4F$, which is calculated by Faraday’s first law. The vertical axis of the Figure is shown by the volumetric gas generation rate of R_gTW_{tot} [Ncm³/s]. Comparatively good agreement is obtained between the experiment data shown by ⊗ and the calculation chain line by $W_{H_2+O_2} = 3I/4F$ for the electrolysis of the KOH solution. It is found that the gas absorption of H₂ and O₂ into the solution is negligibly small.

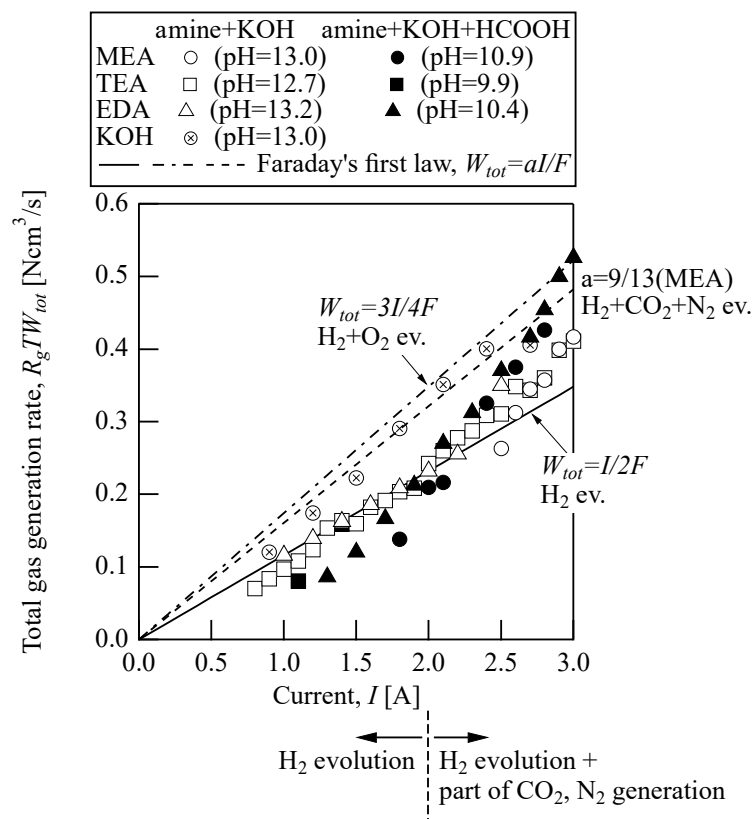


Figure 2. Total gas evolution rates in the electrolysis of several amine solutions, where the initial MEA, TEA and EDA concentrations are set to be 200 g/dm³ regardless of [MEA]₀, [TEA]₀, and [EDA]₀.

On the other hand, when the MEA, TEA and EDA aqueous solutions were electrolyzed, H₂ was generated from the cathode of any amine solution among the six cases regardless of the different pH conditions in a similar way to the KOH solution. However, less or no bubble formation was observed on the anode of the MEA solution, and CO₂ and N₂ bubbles, along with CO or other gas components, were hardly generated from the anode. Small amounts of gas bubbles were observed

only at comparatively higher current conditions of the TEA or EDA solution. The species of evolved gas were identified as CO₂ and N₂ by gas chromatography analysis, and the concentration and the flow rate were determined. Deviations between the MEA data marked by ○ and ● and Faraday's law shown by a broken line ($W_{H_2} = I/2F$) become smaller in the lower current region of $I \leq 2A$, where only H₂ is evolved from the amine aqueous solutions. The same thing holds true in the cases of TEA (□, ■) and EDA (△, ▲). When the current approaches 3 A, the total gas generation rates become slightly larger than the solid line of $W_{tot} = I/2F$. This is because some of the CO₂ and N₂ generated on the anode are discharged after partial absorption into the amine solutions. The total gas evolution rate slightly deviates from the solid line of $W_{tot} = I/2F$ with the increase in the electric current and approaches $W_{tot} = 9I/13F$, as shown by a broken line for the MEA solution. Although the expected asymptote lines are $W_{tot} = 41I/56F$ for TEA and $W_{tot} = 11I/16F$ for EDA, both lines are not shown in the Figure because the differences among the three amine solutions are negligibly small. This tendency is more appreciable for gas rates evolved from the amine solution of the lower pH (pH = 10) than those under the higher pH condition (pH = 13). The condition where the gas evolution rate starts deviating from the solid line of $W_{tot} = I/2F$ in Figure 2 is determined as $I = 2A$ and pH = 10. When $I > 2A$ and pH = 10, CO₂ and N₂ start generating from the anode, and the total gas generation rates approach the broken line of $W_{tot} = 9I/13F$, $W_{tot} = 41I/56F$ or $W_{tot} = 11I/16F$. These results are deeply related to the [OH⁻] concentration in solutions. This is further discussed in the CO₂ gas absorption experiment during electrolysis.

Figure 3 shows experimental results of CO₂ gas dissolution rates in MEA, TEA or EDA + HCOOH aqueous solutions during electrolysis operation. A constant molar fraction and flow rate of CO₂ + Ar gas mixture of $y_{CO_2,in} = 0.373$ and $W_{CO_2,in} = 16.3 \mu\text{mol/s}$ is introduced into the amine aqueous solutions at atmospheric pressure and room temperature ($T = 21 \text{ }^\circ\text{C}$) under a low current condition of 2A. The current condition of $I = 2A$ and the pH = 9 one is selected in such a way that the three amine aqueous solutions still have CO₂ absorption capacity judging from the results of Figure 2. The initial amine concentration, [MEA]₀, [TEA]₀ or [EDA]₀ and the HCOOH concentration before CO₂ introduction, [HCOOH]₀, are given in the Figure. The ratios of the inlet to outlet CO₂ molar fraction for the three amine solutions are obtained as a function of time passage at a constant CO₂ introduction rate of $W_{CO_2,in}$. The $y_{CO_2,out}/y_{CO_2,in}$ ratios on the left-hand side are deeply related to physical-to-chemical CO₂ transitional rates. As shown in Section 2.3, when a conversion rate from a physical absorption state of dissolved CO₂ to a chemical one is fast, the ratio on the vertical axis becomes small. The value on the left-hand side at a steady state is equal to that of $k_{abs}A/(k_1V + k_{abs}A)$. The ratio also depends on the kinds of amines and their pH value. Generally, conversion rates for MEA or EDA solutions are considered to be much faster than those for TEA cases under the same concentration in gram/dm³ units. This is because MEA and EDA are the primary amine solutions and have one or two N-R₁ bonds in an amine molecule. Therefore, they can quickly form their zwitterion states in each molecule, and the transition from the physical state to the chemical one may be enhanced. Each molecule finally dissociates to (C₂H₄OH)NH₃⁺ or (CH₂)₂NH₂H⁺ ions in aqueous solutions. Thus, it is considered that the conversion rate from the physical state to the chemical one for MEA and EDA is faster than that of TEA.

Figure 4 shows $y_{CO_2,out}/y_{CO_2,in}$ values (or the absorption rate) at the steady state for various pH conditions, where the solutions are controlled to [MEA]₀ = 3.10 mol/dm³, [KOH]₀ = 0.18 mol/dm³ and [HCOOH]₀ = 0.15~0.36 mol/dm³. As seen in the Figure, the $y_{CO_2,out}/y_{CO_2,in}$ ratio depends on the pH value, and the ratio becomes smaller with the increase of the pH value. Consequently, the $k_1V/k_{abs}A$ ratio becomes larger at the higher pH value. Since the physical absorption rate constant of k_{abs} may be independent of the amine types, the transition rate constant from a physical state to a chemical one for the MEA electrolyte denoted by k_1 becomes larger with the increase of the pH value. Judging from the slope of the broken line, which means $\frac{(y_{CO_2,out}/y_{CO_2,in})}{[H^+]} = \text{constant}$, the translate rate constant indicated by k_1 may be in proportion to [OH⁻]. Consequently, the relation of $k_1 = 2.5 \times 10^4 \left(\frac{k_{abs}A}{V}\right) [\text{OH}^-]$ is obtained by the comparison between Equation (3) and the broken line in Figure 4. Therefore, the reaction is considered to be the first order with respect to both concentrations of CO₂ and OH⁻. This result leads to the conclusion that Reaction (7) proceeds as R₁NH₂ + CO₂ + OH⁻ ⇌ R₁NCOO⁻ + H₂O, according to the Danckwerts model [12].

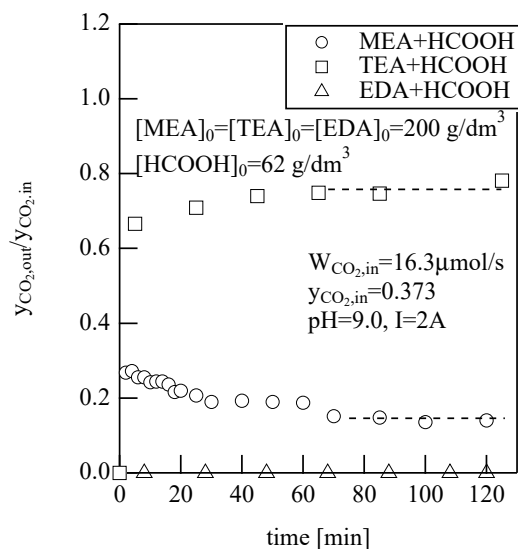


Figure 3. Rates of CO₂ absorption into three amine aqueous solutions. The gram concentration of [MEA]₀, [TEA]₀ or [EDA]₀ is 200 g/dm³.

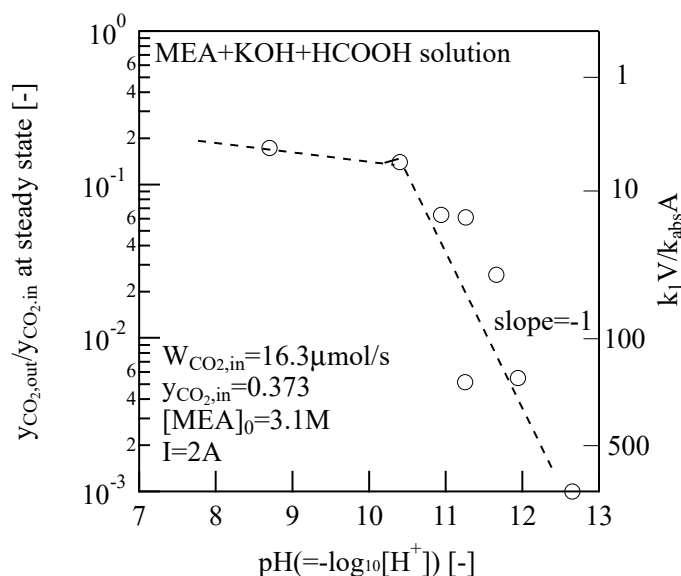


Figure 4. Relation of CO₂ absorption rate as a function of H⁺ ion concentration.

The overall resistivities of the MEA solutions were determined from the relation between the electric potential and the current during electrolysis. Figure 5 shows variations of the overall resistivity of several amine solutions as a function of the current. The overall resistivities, ρ , are determined using the relation of $\rho = \frac{A}{I} \frac{dE}{dI}$. Judging from the experimental relation between I and E , the resistivities of the three amine solutions show almost constant values except for the very low current region. As seen in the Figure, the resistivities of the MEA and EDA aqueous solutions are slightly lower than that of the TEA one, having the same concentration in g/dm³ unit. The difference between the KOH solution (the broken line) and any amine solution is caused by other ions dissolved in each aqueous solution. The broken line in Figure 5 shows a theoretical resistivity based on the strong electrolyte model, which is determined by the law of Kohlrausch's independent ionic migration and is described by $\Lambda^\infty = z_1 \Lambda_1^\infty + z_2 \Lambda_2^\infty$ for two-component infinite diluted solution mixtures. The broken line for the KOH solution is calculated using $z_1 = 1$ and $\Lambda_1^\infty = 0.073 \text{ Sm}^2/\text{mol}$ for the K⁺ ion and $z_2 = 1$ and $\Lambda_2^\infty = 0.199 \text{ Sm}^2/\text{mol}$ for OH⁻. A comparatively good agreement is obtained between the experimental data of the KOH solution and its theory. In addition, the Kohlraushu's square root law also predicts the relation of $\Lambda = \Lambda^\infty - k\sqrt{C}$. Therefore, the overall resistivities of MEA, EDA and TEA solutions increase with the increase in the total ion concentrations involved in the solution, denoted by C . Figure 6 shows a correlation of experimental resistivities at

$I = 3A$ for the three amine solutions as a function of the pH value. Any of the three amine solutions show similar variations with the pH value, and the resistivity becomes lower at higher pH values. It is noticed that the TEA solutions show comparatively higher resistivity values than other amines, regardless of the pH values. The C values are considered to become larger with the decrease in the pH values because of a greater amount of CO_2 absorption and, consequently, more CO_3^{2-} , HCO_3^- , R_1NHCO_2 and $R_1NH_3^+$ ions generated.

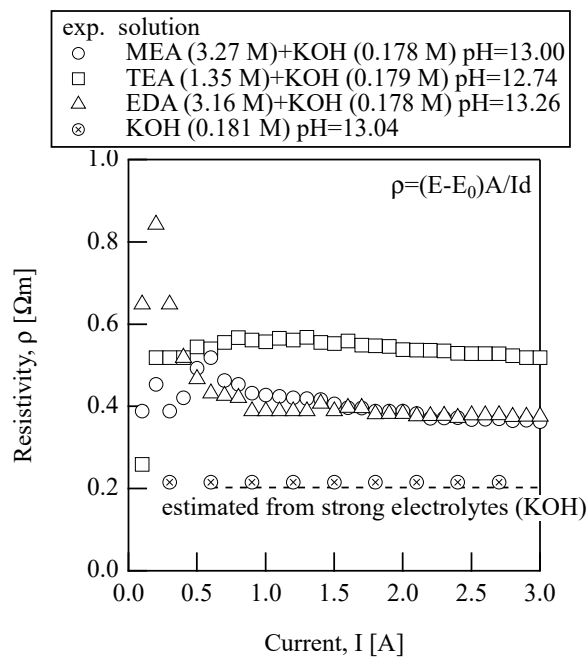


Figure 5. Resistivity of MEA aqueous solutions as a function of current.

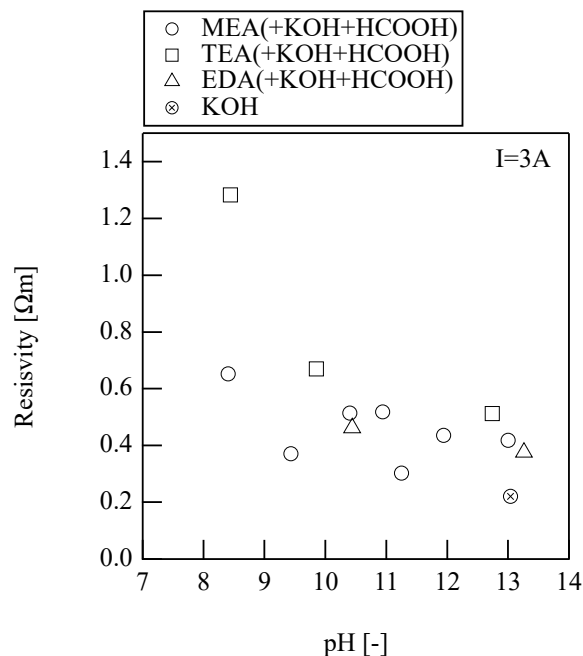


Figure 6. Relation between resistivity and pH for aqueous MEA, TEA and EDA solutions at comparatively high current conditions, where $[MEA]_0 = 3.1 M$, $[TEA]_0 = 1.4 M$, $[EDA]_0 = 3.2 M$, $[KOH]_0 = 0.18 M$, and $[HCOOH] = 0.15\sim 0.36 M (mol/dm^3)$.

As already known in previous studies, CO_2 is chemically absorbed in the MEA aqueous solutions with the two types of bicarbonate (HCO_3^-) and carbamate (R_1NHCOO^-) [20]. Since

two valences of MEA are necessary in order to form one carbamate, the maximum CO_2 loading becomes $0.5 \text{ mol-CO}_2/\text{mol-amine}$. On the other hand, one TEA molecule changes one bicarbonate of the potential maximum loading, which corresponds to a $1 \text{ mol-CO}_2/\text{mol-amine}$. Figure 7 shows calculative variations of respective ion concentrations for the $\text{R}_1\text{NH}_2 + \text{KOH}$ aqueous solution with the increase in CO_2 loading, where the initial concentrations of $[\text{R}_1\text{NH}_2]_0 = 0.1 \text{ mol/dm}^3$ and $[\text{KOH}]_0 = 0.1 \text{ mol/dm}^3$ are assumed. The increase in $[\text{CO}_2]_0$ results in the increase of $[\text{H}^+]$ and also in the increase of $[\text{HCO}_3^-]$, $[\text{CO}_3^{2-}]$, $[\text{R}_1\text{NHCO}_2^-]$ and $[\text{R}_1\text{NH}_3^+]$. However, $[\text{CO}_3^{2-}]$ and $[\text{R}_1\text{NHCO}_2^-]$ start decreasing at a higher loading point than the location of $[\text{CO}_2]_0 = 0.1$. $[\text{CO}_3^{2-}]$ is the main CO_2 absorption ion when pH is high. The concentrations for the $\text{R}_3\text{N} + \text{KOH}$ (TEA) aqueous solution behave in a similar way to MEA. When CO_2 loading is small, or the pH value is high, the main ion species are CO_3^{2-} . The ethanol carbamate ion concentration of $\text{R}_1\text{NHCO}_2^-$ becomes the major one around $[\text{CO}_2]_0 = 0.1 \text{ mol/dm}^3$ with the increase in CO_2 loading. Further CO_2 loading results in the fact that the major species in the MEA solution become R_1NH_3^+ and HCO_3^- .

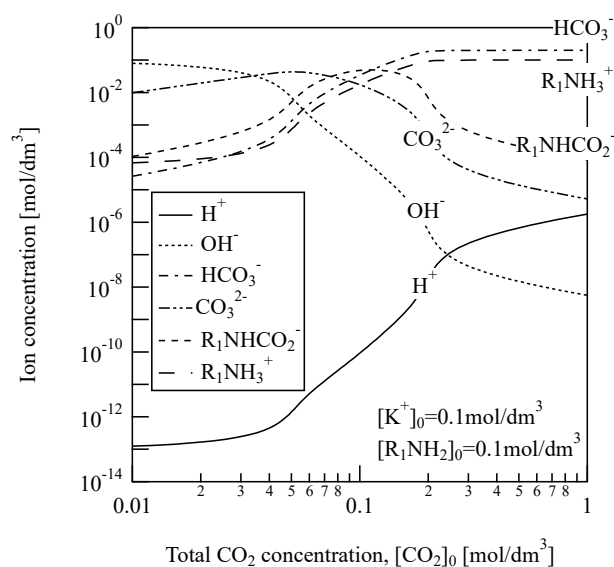


Figure 7. Variations of calculated ion concentration in aqueous MEA + KOH solution with CO_2 loading.

The conditions to select which amine solution is preferable for selective H_2 evolution by electrolysis are to show (1) similar electric conductivity to that of the KOH alkali solution, (2) selective H_2 evolution and CO_2 absorption during electrolysis, and (3) sufficient CO_2 absorption rate and capacity during electrolysis. All those results show that the MEA or EDA solutions can serve as an appropriate electrolyte for selective H_2 generation by electrolysis under a current condition of $I \leq 2 \text{ A}$ ($=11.3 \text{ mA/cm}^2$) and a pH condition of $\text{pH} \geq 10$. It is preferable to use the MEA solution for electrolytes because EDA absorbs CO_2 irreversibly, and the CO_2 absorption rate of TEA is lower than others. Figure 8 shows a schematic diagram of the continuous MEA electrolysis system to provide selective H_2 evolution and CO_2 recovery. The pH condition can be controlled by KOH and HCOOH . A combination of electrolysis of the MEA alkali solution and reversible CO_2 absorption in/desorption from the electrolyte can lead to selective H_2 generation. The CO_2 desorption will be performed using a regeneration tower heated to $100\text{--}140 \text{ }^\circ\text{C}$ [21]. Although CO_2 and N_2 are generated from an anode, CO_2 generated can be immediately absorbed in amine solutions, and effective separation can be performed. The CO_2 absorption is the first order with respect to the OH^- concentration in solute. Since the pH value decreases with the progress of CO_2 absorption, the pH control by CO_2 desorption is necessary for the long-time electrolysis operation. A small amount of N_2 is physically absorbed in the solution, and the rest is generated from the anode. The electrolysis of amine solutions, along with CO_2 capture [10,11], can be understood by the physical absorption process and the chemical equilibrium conditions of reactions among related ions.

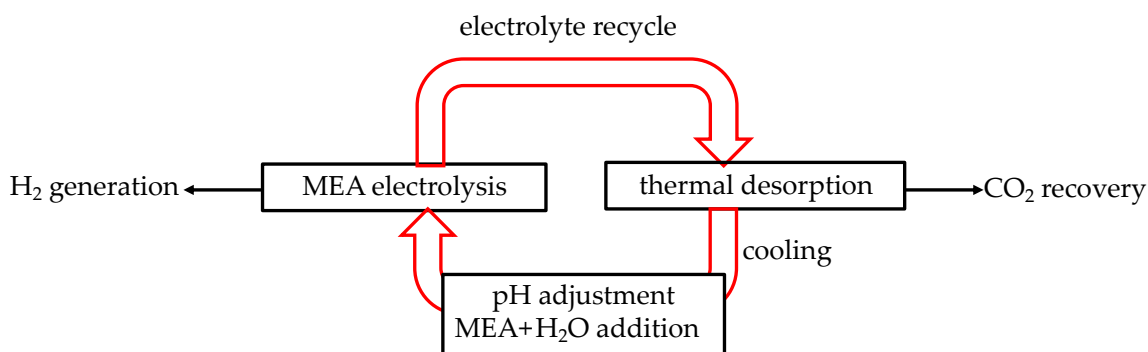


Figure 8. Continuous H₂ generation system using MEA electrolyte.

5. Conclusions

H₂ generation on the cathode and CO₂ absorption on the anode were observed during electrolysis of MEA, TEA and EDA aqueous solutions under high pH conditions of pH > 10. The H₂ evolution rates are correlated by Faraday's first law. No, or smaller amounts of CO₂ bubbles than stoichiometric values, evolved in the three amine solutions because of selective CO₂ absorption into amine solutions. The CO₂ dissolution rate is in proportion to [CO₂] and [OH⁻], and the CO₂ chemical absorption rates for MEA and EDA are faster than that of TEA because of the presence of the N–H bond in MEA and EDA. Overall resistivities of the three amine aqueous solutions are determined and correlated as a function of the [H⁺] or [OH⁻] concentration. The resistivities of MEA solutions are kept low under high pH conditions and increase with the decrease in the pH values. This is because of the increase in the CO₂ concentration in MEA solution, where ions, such as [CO₃²⁻], [HCO₃⁻], [R₁NHCO₂⁻] and [R₁NH₃⁺], are chemically absorbed. A combination of electrolysis of the MEA alkali solution and CO₂ desorption from the electrolyte can provide a continuous way to produce H₂.

Author Contributions: All authors contributed to the investigation. Conceptualization, S.F. and R.S.; Methodology, M.O.; GC analysis, K.K.; Data interpretation, S.F. and R.S.; Resources, S.F., R.S., M.O. and K.K.; Software, S.F. and M.O.; Writing—original draft preparation, S.F., R.S. and K.K. All authors have read and agreed to the published version of the manuscript.

Funding: This research received no external funding.

Data Availability Statement: The data presented in this study are available on request from the corresponding author.

Acknowledgments: The authors extend their appreciation to E-plus Co., Ltd. for preparing the electrolysis reactor used in the present study.

Conflicts of Interest: The authors declare no conflict of interest.

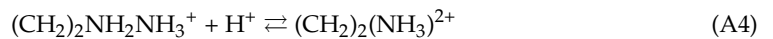
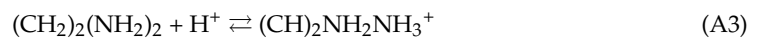
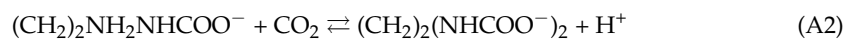
Nomenclature

<i>A</i>	total bubble surfaces in solution [m ²]
<i>a</i>	mean ionic diameter [m]
<i>C</i>	total ion concentration [mol/dm ³]
<i>E</i>	electric potential, voltage [V]
<i>F</i>	Faraday's constant (=9.648 × 10 ⁴) [C/mol]
<i>f_i</i>	activity coefficient of <i>i</i> component ion dissolved in solution [-]
<i>I</i>	current [A]
<i>J</i>	ionic strength of solution [mol/dm ³]
<i>K_i</i>	equilibrium constant of reaction <i>i</i> [-] or [(mol/dm) ^{<i>n</i>}]
<i>k</i>	constant [m ^{3.5} /mol ^{1.5} Ω]
<i>k_{abs}</i>	mass-transfer coefficient through boundary layer around bubbles [m/s]

k_1	the first-order reaction rate constant from physical solution state to chemical solution one [1/s]
k_2	second-order reaction rate constant [dm^3/mols]
l	distance between two electrodes [m]
N	the total number of ion species dissolved in solution [-]
p_{CO_2}	CO_2 partial pressure [Pa]
V	liquid electrolyte volume [m^3]
W	evolution rate of gas [mol/s] or [Nm^3/s]
y_{CO_2}	molar fraction of CO_2 in gas phase [-]
z	ionization degree in solution [-]
Λ	molar conductivity [$\text{m}^2/\text{mol}\Omega$]
ρ_k	electric resistivity of component k [Ωm]
$[]$	molar or gram concentration in solution [mol/dm^3] or [g/dm^3]
$[]_0$	molar or gram concentration in solution at initial condition [mol/dm^3] or [g/dm^3]

Appendix A. EDA Solution

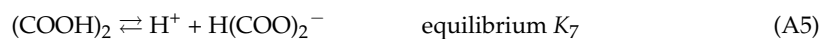
When EDA of $(\text{CH}_2)_2(\text{NH}_2)_2$ is used for an electrolyte in place of MEA or TEA aqueous solution, it reacts with CO_2 and H^+ ions dissolved in the aqueous solution. Then, the following reactions may progress in place of Equations (4) and (5):



The kinds of ions involved in solutions are H^+ , $(\text{CH}_2)\text{NH}_2\text{NHCOO}^-$, $(\text{CH}_2)_2(\text{NHCOO}^-)_2$, $(\text{CH}_2)_2\text{NH}_2\text{NH}_3^+$, $(\text{CH}_2)_2(\text{NH}_3)^{2+}$ and may be present according to various pH values.

Appendix B. $(\text{COOH})_2$ Solution

When the oxalic acid $(\text{COOH})_2$ is used for the pH control in place of the formic acid HCOOH , the following equilibrium reactions progress in place of Equation (6):



$$K_7 = \frac{f_{\text{H}^+} [\text{H}^+] f_{\text{H}(\text{COO})_2^-} [\text{H}(\text{COO})_2^-]}{f_{(\text{COOH})_2} [(\text{COOH})_2]} = 10^{-1.04} \quad (\text{A7})$$

$$K_8 = \frac{f_{\text{H}^+} [\text{H}^+] f_{(\text{COO})_2^{2-}} [(\text{COO})_2^{2-}]}{f_{\text{H}(\text{COO})_2^-} [\text{H}(\text{COO})_2^-]} = 10^{-3.82} \quad (\text{A8})$$

The molar concentrations of MEA and CO_2 in the aqueous solution depend on only $[\text{H}^+]$. Therefore, the results do not depend on which of $(\text{COOH})_2$ or HCOOH is used for the acid control.

References

- Ng, W.K.; Wong, W.Y.; Rosli, N.A.; Loh, K.S. Commercial anion exchange membranes (AEMs) for fuel cell and water electrolyzer applications: Performance, durability and materials advancement. *Separations* **2023**, *10*, 424. [[CrossRef](#)]
- Wang, S.; Lu, A.; Zhong, C.J. Hydrogen production from water electrolysis: Role of catalysts. *Nano Converg.* **2021**, *8*, 4. [[CrossRef](#)] [[PubMed](#)]
- Schalenbach, M.; Zeradjanin, A.R.; Kasian, O.; Chervko, S.; Mayrhofen, K.J.J. A perspective on low-temperature water electrolysis challenges in alkaline and acidic technology. *Int. J. Electrochem. Sci.* **2018**, *13*, 1173–1226. [[CrossRef](#)]
- Chen, L.; Dong, X.; Wang, Y.; Xia, Y. Separating hydrogen and oxygen evolution in alkaline water electrolysis using nickel hydroxide. *Nat. Commun.* **2016**, *7*, 11741. [[CrossRef](#)] [[PubMed](#)]

5. Mohamadbigy, K.H.; Bazmi, M.; Behradi, R.; Binesh, R. Amine absorption column design using mass transfer rate simulation. *Pet. Coal* **2005**, *47*, 39–46. Available online: <https://www.researchgate.net/publication/237642937> (accessed on 16 November 2023).
6. Teranishi, K.; Ishikawa, A.; Nakai, H. Computational chemistry studies on CO₂ chemical absorption technique: Challenge on energy and environmental issues. *J. Comput. Chem. Jpn.* **2016**, *15*, A15–A29. [[CrossRef](#)]
7. Suda, T.; Iwaki, T.; Mimura, T. Facile determination of dissolved species in CO₂-amine-H₂O system by NMR spectroscopy. *Chem. Lett.* **1996**, *25*, 777–778. [[CrossRef](#)]
8. Li, L.; Maeder, M.; Burns, R.; Puxty, G.; Clifford, S.; Yu, H. The Henry coefficient of CO₂ in the MEA-CO₂-H₂O system. *Energy Procedia* **2017**, *114*, 1841–1847. [[CrossRef](#)]
9. Sato, K.; Hamada, S.; Isaka, M.; Nishimura, T.; Ashikawa, M.; Robert, M.; Usui, T. Reprocessing wastewater by electrolysis. *Proc. Sanit. Eng. Symp.* **2000**, *8*, 28–33. Available online: <http://hdl.handle.net/2115/7203> (accessed on 16 November 2023).
10. Hack, J.; Maeda, N.; Meier, D.M. Review on CO₂ capture using amine-functionalized materials. *ACS Omega* **2022**, *7*, 39520–39530. [[CrossRef](#)] [[PubMed](#)]
11. Yamada, H. Amine-based capture of CO₂ for utilization and storage. *Polym. J.* **2021**, *53*, 93–102. [[CrossRef](#)]
12. Danckwerts, P.V. The reaction of CO₂ with ethanolamines. *Chem. Eng. Sci.* **1979**, *34*, 443–446. [[CrossRef](#)]
13. Knuutila, H.; Juliussen, O.; Svendsen, H.F. Kinetics of the reaction of carbon dioxide with aqueous sodium and potassium carbonate solution. *Chem. Eng. Sci.* **2010**, *65*, 6077–6088. [[CrossRef](#)]
14. Suib, S.L. *New and Future Developments in Catalyst: Activation of Carbon Dioxide*; Elsevier: Amsterdam, The Netherlands, 2013; p. 163. [[CrossRef](#)]
15. Hagewiesche, D.P.; Ashour, S.S.; Al-Ghawas, H.A.; Sandall, O.C. Absorption of carbon dioxide into aqueous blends of monoethanolamine and N-methyldiethanolamine. *Chem. Eng. Sci.* **1995**, *50*, 1071–1079. [[CrossRef](#)]
16. Aboudheir, A.; Tontiwachwuthikul, P.; Chakma, A.; Idem, R. Kinetics of the reactive absorption of carbon dioxide in high CO₂-loaded, concentrated aqueous monoethanolamine solutions. *Chem. Eng. Sci.* **2003**, *58*, 5195–5210. [[CrossRef](#)]
17. Donaldson, T.L.; Nguyen, Y.N. Carbon dioxide reaction kinetics and transport in aqueous amine membrane. *Ind. Eng. Chem. Fundam.* **1980**, *19*, 260–266. [[CrossRef](#)]
18. Dean, J.A. *Lange's Handbook of Chemistry*, 12th ed.; McGraw Hill: New York, NY, USA, 1979; pp. 4–9, ISBN 0-07-016384-7.
19. Wright, M.R. *An Introduction to Aqueous Electrolyte Solutions*; Wiley: Hoboken, NJ, USA, 2007; ISBN 978-0-470-84293-5.
20. Horng, S.Y.; Li, M.H. Kinetics of absorption of carbon dioxide into aqueous solutions of monoethanolamine + triethanolamine. *Ind. Eng. Chem. Res.* **2002**, *41*, 257–266. [[CrossRef](#)]
21. Rao, A.B.; Rubin, E.S. A technical, economic and environmental assessment of amine-based CO₂ capture technology for power plant greenhouse gas control. *Environ. Sci. Technol.* **2002**, *36*, 4467–4475. [[CrossRef](#)] [[PubMed](#)]

Disclaimer/Publisher's Note: The statements, opinions and data contained in all publications are solely those of the individual author(s) and contributor(s) and not of MDPI and/or the editor(s). MDPI and/or the editor(s) disclaim responsibility for any injury to people or property resulting from any ideas, methods, instructions or products referred to in the content.